Geophysical Research Letters

RESEARCH LETTER
10.1029/2025GL119801

SWOT Sheds Light on Seiche Oscillations Within Atoll Islands

E. Rebouillat[1], L. Oruba[2], M. Hopuare[1], S. Planes[3], and E. Dormy[4]

[1]GEPASUD, Université de la Polynésie Française, Puna'auia, French Polynesia, [2]Laboratoire Atmosphères, Observations Spatiales (LATMOS), Sorbonne Université, UVSQ, CNRS, Paris, France, [3]CRIOBE/USR 3278, CNRS-EPHE-UPVD, Moorea, French Polynesia, [4]Département de Mathématiques et Applications, Ecole Normale Supérieure, CNRS, PSL University, Paris, France

Key Points:

- Seiche-like structures are captured by SWOT-KaRIn Sea Surface Height (SSH) anomaly fields in French Polynesia lagoons
- SWOT SSH anomaly observations reveal similar seiche geometries as eigenmodes computed using a shallow-water model
- In situ wave measurements in the Raroia atoll lagoon confirm the presence of seiche modes

Supporting Information:

Supporting Information may be found in the online version of this article.

Correspondence to:

L. Oruba and E. Dormy,
ludivine.oruba@latmos.ipsl.fr;
emmanuel.dormy@ens.fr

Citation:

Rebouillat, E., Oruba, L., Hopuare, M., Planes, S., & Dormy, E. (2026). SWOT sheds light on seiche oscillations within atoll islands. *Geophysical Research Letters*, *53*, e2025GL119801. https://doi.org/10.1029/2025GL119801

Received 6 OCT 2025
Accepted 1 FEB 2026

Abstract This study investigates the occurrence of surface elevation oscillations, known as seiches, at the atoll scale. We show that the innovative Ka-band Radar Interferometer (KaRIn) onboard the Surface Water Ocean Topography (SWOT) satellite makes it possible to visualize seiche-like structures within lagoons of French Polynesia. This ability to capture two-dimensional sea surface undulations of low amplitude (on the order of a few centimeters) in relatively small water bodies (less than 80 km in length) is unprecedented in satellite altimetry, and opens new avenues of research into these events and their contribution to coastal erosion and flooding. Our study combines sea surface height observations from SWOT with in situ measurements conducted in the Raroia lagoon and theoretical calculations based on an eigenvalue model. These three complementary approaches—satellite remote sensing, in situ data, and theoretical modeling—allow us to investigate both the spatial and spectral properties of seiches in atoll islands.

Plain Language Summary In closed or semi-enclosed water bodies, a resonant phenomenon can happen in which the water surface performs standing oscillations. These oscillations, known as *seiches*, have well-defined periods and geometries at the basin scale. Here we investigate their presence in the lagoon of atoll islands using in situ measurements, modeling, and the Surface Water Ocean Topography (SWOT) mission, a new satellite that provides for the first time two-dimensional images of the ocean surface elevation with an unprecedented precision and resolution. We show that SWOT does capture seiche-like structures, and our in situ measurements confirm that such resonant modes do occur in the lagoon of Raroia. This is a first step toward understanding and assessing the importance of these modes in Pacific atoll islands, where they have received relatively little attention though they appear to play a role in sediment transport and submersion events.

1. Introduction

In the present study, we investigate surface seiches in tropical atoll islands. Surface seiches correspond to standing, long-period, surface gravity waves that can arise in closed or semi-enclosed water bodies; so far, they have been studied in lakes, harbors and bays but received no or little attention at the scale of atoll islands. Usually ranging a few centimeters to decimeters, they can reach higher amplitudes under some extreme weather conditions. Seiche amplitudes depend on basin resonance properties (bathymetry, friction) and external forcing, including atmospheric and oceanic disturbances, or earthquakes. The forcing can trigger free or forced seiches (e.g., Wilson, 1972), with exceptional intensities when the frequencies of forcing and basin resonance are aligned (Rabinovich, 2009). Strong events may cause flooding and intense currents (Bechle et al., 2015), disrupt navigation, and contribute to erosion or sediment resuspension (e.g., Seo et al., 2024).

Few studies looked at surface (barotropic) seiches from satellite observations. Matson and Berg (1981) reported probably the first indirect satellite observation of seiches based on radiometer measurements in Great Salt Lake. Metzner et al. (2000) observed seiches in the Baltic Sea using along-track radar altimetry. Zheng et al. (2014) used L4 gridded altimetry products to study seiche modes in the South China Sea, with wavelengths ranging between 300 and 500 km. More recently, a direct observation of seiches using the Surface Water Ocean Topography (SWOT) satellite was performed by Monahan et al. (2025) in the Dickson fjord in Greenland.

Only very few studies mention fully two-dimensional seiches at the scale of atoll islands, with lagoons extending over a few 10-km and depth of several 10-m. At the local scale of a few 100-m, there are several studies of one-dimensional (cross-shore) resonant wave patterns over fringing reef flats forced by infragravity waves

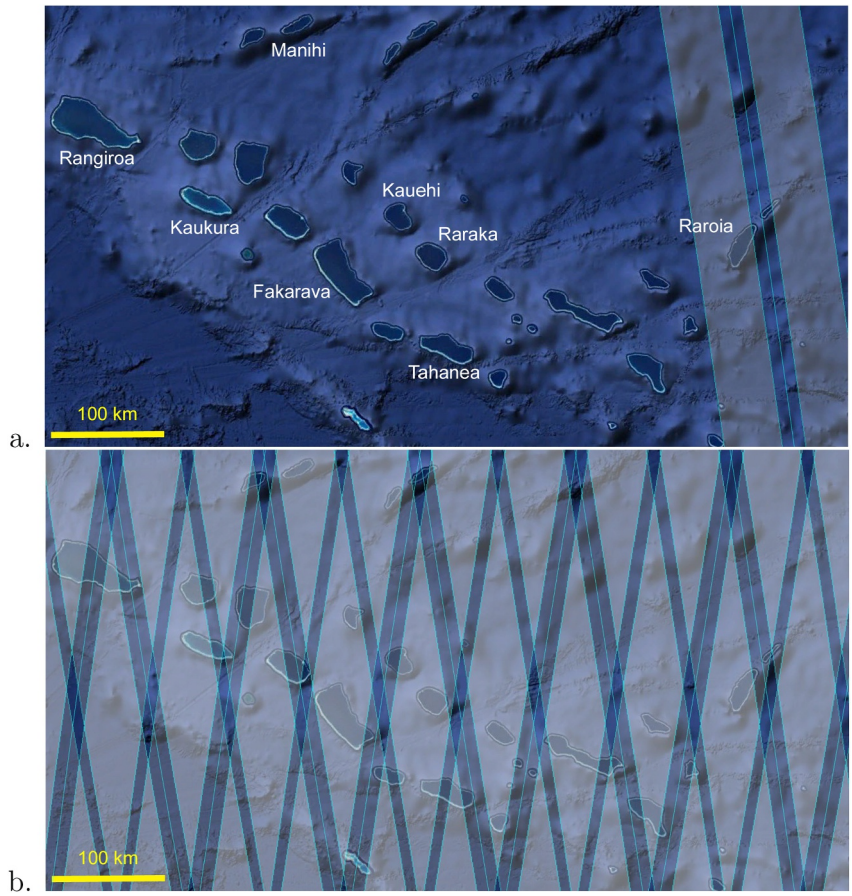

Figure 1. Location of the atolls shown in Figure 2 superimposed to the KaRIn swath (transparent white), which spans 60 km on both sides of nadir (highlighted in cyan) and includes a nadir gap, during the 1-day (a) and 21-day (b) orbits of SWOT. Map coverage: S14°15′–S17°35′, W148°00′–W141°30′.

(e.g., Cheriton et al., 2016; Gawehn et al., 2016; Péquignet et al., 2009; Pomeroy et al., 2012; Shimozono et al., 2015). At a somewhat larger scale, local alongshore standing wave patterns of infragravity waves refracted by the presence of the nearshore reef were identified by Winter et al. (2017), and stationary very low frequency waves were identified by Sous et al. (2019). However, regarding measurements of seiches at atoll scale, we are only aware of the work of Lenhardt (1991) in the lagoon of Tikehau in French Polynesia, who measured seiche modes of 50-min period, less than 0.5-cm high and lasting a day or more.

French Polynesia is located in the South Pacific. The atolls studied in this article are shown in Figure 1. Among them, Rangiroa is the largest (approximately 80 km long, 32 km wide), while Manihi is the smallest (27 km by 8 km). Due to their spatial resolution on the order of several tens of kilometers, classical gridded altimetry products cannot capture the spatial variability of the Sea Surface Height (SSH) inside such lagoons. However, spatial variations in SSH at the lagoon scale can now be captured by the SWOT satellite, launched in December 2022, thanks to its innovative Ka-band Radar Interferometer (KaRIn) (e.g., Fu et al., 2024; Morrow et al., 2019). Unlike classical altimeters limited to 1D along-track profiles, SWOT provides 2D SSH observations up to 250 m resolution in two 50 km-wide swaths, separated by a 10 km nadir gap. From December 2022 to July 2023, SWOT operated in a fast-sampling Calibration-Validation (Cal/Val) orbit with near-daily repeat cycles. Since July 2023, it has been on its nominal (Science) orbit, offering near-global coverage every 21 days.

In this study, we combine altimetry data from SWOT, theoretical modeling, and in situ measurements by pressure sensors deployed in the Raroia lagoon, which has the particularity of being located within a SWOT swath along the Cal/Val orbit (Figure 1a). We equipped this atoll with 9 pressure sensors to retrieve the water height within the lagoon and outside the barrier reef during SWOT's Cal/Val phase.

2. Data and Methods

2.1. Dedicated SWOT SSH Anomaly

The present study relies on KaRIn Low Rate SSH products. We use the L3 Unsmoothed version 2.0.1 data set, provided on a grid with 250-m resolution, to compute images of the SSH anomalies in the lagoons and investigate the presence of seiches. The SSH anomaly included in the L3 product is unreliable in lagoons due to the limited accuracy of geophysical models (especially the hydrodynamic and geoid models) in such small-scale environments. We thus constructed a SSH anomaly field dedicated to the investigation of seiches in lagoons. L3 product fields are combined to remove the effects of solid Earth tide, pole tide and load tide. However, ocean tide correction, internal tide correction, and dynamic atmospheric correction (DAC) were omitted over atoll lagoons. The MSS (Mean Sea Surface) correction as provided in the SWOT L3 product was also omitted. Instead, the mean value of the thus-obtained field, computed over all available cycles (97 during Cal/Val and up to 29 Science cycles to date), is subtracted as an estimate of the mean sea level (see Text S2 in Supporting Information S1 for more details).

2.2. Shallow-Water Eigenmodes

Seiches are characterized by the period and geometry of the free surface oscillations. To determine the first seiche modes, we build a shallow water model formulated as an eigenvalue problem. The wavelength of the first resonant modes is indeed on the order of the lagoon's size, that is a few dozen kilometers, while its depth is only a few dozen meters; the shallow water approximation is thus fully justified. Details of the model construction are available in Text S1 in Supporting Information S1. The model relies on a bathymetry to compute the eigenmodes $V_i(x, y)$, which describe the spatial geometry of the seiche modes, along with the corresponding oscillation periods T_i derived from the eigenvalues. The eigenmodes are sorted by decreasing period.

Very few lagoons in French Polynesia are fully covered by bathymetric data (e.g., Andréfouët et al., 2020). When no bathymetry is available, a constant depth model with lagoon boundaries provided by the open public data platform *TeFenua* was used (see https://arcg.is/0jP5u00 and Andréfouët et al., 2005, for more details). Audusse et al. (2017) have shown that the solution of the eigenmode problem with constant depth (i.e., the Helmholtz equation) provides a good approximation at leading order of the modes with mild-slope variations (see also Levitin et al., 2023). The eigenmodes of the aforementioned lagoons have thus been computed numerically using either constant bathymetry or bathymetric data; the structures of the first four eigenmodes from both methods are remarkably similar (see Figures S2 and S3 in Supporting Information S1).

2.3. Spectral Analysis of Pressure Sensor Data

The Raroia atoll was instrumented with 9 underwater pressure sensors (OSSI-010-022 Wave Gauge Blue and RBR Solo Depth), 7 of which were placed within the lagoon and 2 on the fore reef. They were deployed at approximately 10 m depth, recording the relative pressure at 1 Hz. The Fast Fourier Transform algorithm, applied to the detrended pressure signal recorded between 2 April and 9 June 2023, provides an estimate of the power spectral density, denoted $E(f)$ (in units of $m^2 \cdot s$), after correcting for depth attenuation. The significance of the spectral peaks is confirmed using a Welch's overlapped segment averaging estimator and confidence intervals (Emery & Thomson, 2001) (see Figure S7 in Supporting Information S1).

Further information on the geometry of the modes of oscillation can be obtained through Continuous Wavelet Transform (CWT). The CWT computation is performed using a filterbank of 48 Morse wavelets per octave, spanning frequencies from 0.025 to 100 Hz. This range corresponds to the estimated seiching frequency band predicted by our model for the Raroia lagoon. The Morse wavelets are defined with a symmetry parameter of 3 and a time-bandwith product of 120. The CWT is used to infer seiche geometries by analyzing phase lags between sensors within the seiching frequency band. Phase lags between two sensors P_i and P_j are defined as

$$\phi_{i,j}(f,t) = \arg(\mathrm{CWT}_i(f,t)) - \arg(\mathrm{CWT}_j(f,t)) \qquad [2\pi], \tag{1}$$

where arg denotes the argument of the complex CWT.

2.4. Reliability of SWOT Measurements in Lagoons

To assess the reliability of KaRIn measurements in lagoons, a comparison with the pressure sensor measurements in Raroia during the Cal/Val phase is performed. Such a comparison is not straightforward as the two devices rely on fundamentally different measurement approaches.

The satellite and the pressure sensors do not capture the same geophysical effects: unlike satellites, the pressure sensors (being fixed on the seafloor) are not affected by solid earth motions and they do not capture the inverse barometer effect. The SSH anomaly constructed as described in Section 2.1 (see also Text S2 in Supporting Information S1) is thus compared to the relative water level reconstructed from the pressure recordings, after correcting for depth attenuation and adding the inverse barometer effect. Satellite and in situ measurements are collocated both in space and time. The collocation in time includes moving averages of the in situ recordings as an attempt to get rid of the wavelengths smaller than the satellite product grid size, which are not captured by the satellite due to the limited spatial resolution (see Text S3 in Supporting Information S1 for more details). Timeseries corresponding to the difference between satellite and in situ water level measurements can be derived for each sensor. The root mean square (RMS) value of these differences is on the order of 2–3 cm within the lagoon, both for the 2-km and 250-m SWOT products, highlighting SWOT's ability to capture centimeter-scale sea level variations within lagoons (see Table S2 in Supporting Information S1).

3. SWOT Observations of Seiches in French Polynesia Lagoons

Seiches in lagoons are first investigated by analyzing the SSH anomalies computed as described in Section 2.1 (see also Text S2 in Supporting Information S1). We use the 29 KaRIn cycles available to date from the SWOT Science orbit, and focus on images of large enough lagoons with no major islands or islets, to ensure a sufficient resolution of the lagoon images and to minimize potential land contamination in the signal. A selection of 12 of those images is presented in Figure 2, showing the SSH anomaly field over the 7 atolls highlighted in Figure 1, ordered by decreasing lagoon size (see also Table S1 in Supporting Information S1). Striking seiche-like structures are noticeable on these images. Several different large-scale geometries, more or less complex, can be identified for a single lagoon, especially for the two largest atolls (see Figures 2a–2f). The crest-to-trough amplitude of these SSH anomaly patterns varies up to 6 cm. These structures are also visible in the 2-km KaRIn products (not shown here).

The features revealed in Figure 2 can be compared to the eigenmodes computed using a shallow water model (see Section 2.2). Figure 3 compiles the eigenmodes V_i derived from the model, with geometries similar to the patterns highlighted in Figure 2. A panel-by-panel comparison of Figures 2 and 3 highlights the strong similarity of the patterns observed by SWOT and seiche modes. Also, as expected for seiche modes, we observe that the amplitude of the first seiche mode (Figures 2a, 2d, 2g, 2j, and 2k) is larger than that of higher-order modes, especially for smaller lagoons (Figures 2h, 2i, and 2l).

SWOT can only provide a snapshot of the spatial structure of seiches. A more comprehensive description requires in situ measurements to assess their temporal dynamics. The next section is thus dedicated to the Raroia lagoon.

4. Case Study of the Raroia Atoll

The 9 pressure sensors deployed in Raroia allow for a spectral characterization of seiches. Although the measurements are spatially localized, comparing the signals recorded at different locations provides some insight into the spatial structure of the seiche modes.

A first characterization of the seiche modes captured by the pressure sensors is performed using Fourier analysis (see Section 2.3). Figures 4a–4d compare power spectral density estimates derived from ocean (Figure 4a) and lagoon (Figures 4b, 4c, and 4d) sensors within the $12 - 78$ min band (spectra over a period range from 10 s to 27 hr are available in Figure S5 in Supporting Information S1). Unlike the ocean spectrum, the lagoon spectra exhibit long-period localized energy peaks, which match the computed seiche modes.

The first seiche modes are computed using the shallow-water model based on the bathymetry product available for Raroia (see Section 2.2). Their corresponding periods consistently align with the energy peaks observed in the lagoon wave gauge spectra (Figure 4g). The geometries of the first 4 modes computed from the model are shown in Figures 5a–5d, superimposed to the wave gauge locations. The spectral content of the wave gauges corroborates the

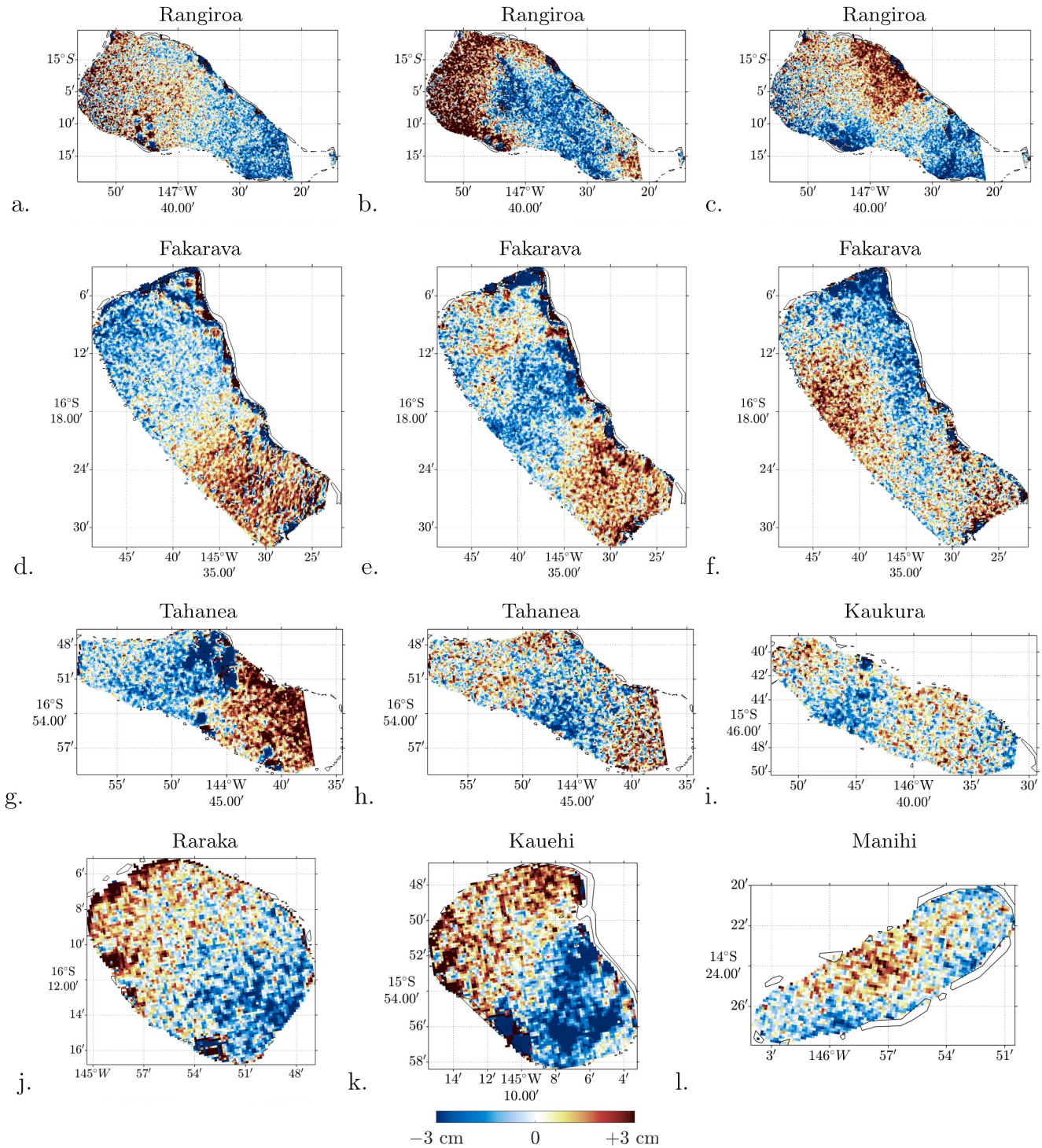

Figure 2. Sea Surface height anomaly reconstructed from SSH KaRIn measurements in the lagoons of (a–c) Rangiroa, (d–f) Fakarava, (g–h) Tahanea, (i) Kaukura, (j) Raraka, (k) Kauehi and (l) Manihi. Each colorbar is centered on the median value inside the lagoon and spans a range of 6 cm.

nodal line positions: spectra from gauges located on nodal lines lack the energy peaks associated to the corresponding seiche modes. For instance, Figure 4b, showing the spectrum from P_3, displays all four peaks associated with the first four modes. In contrast, the 34-min and 20-min peaks, corresponding to modes 2 and 4, are absent from

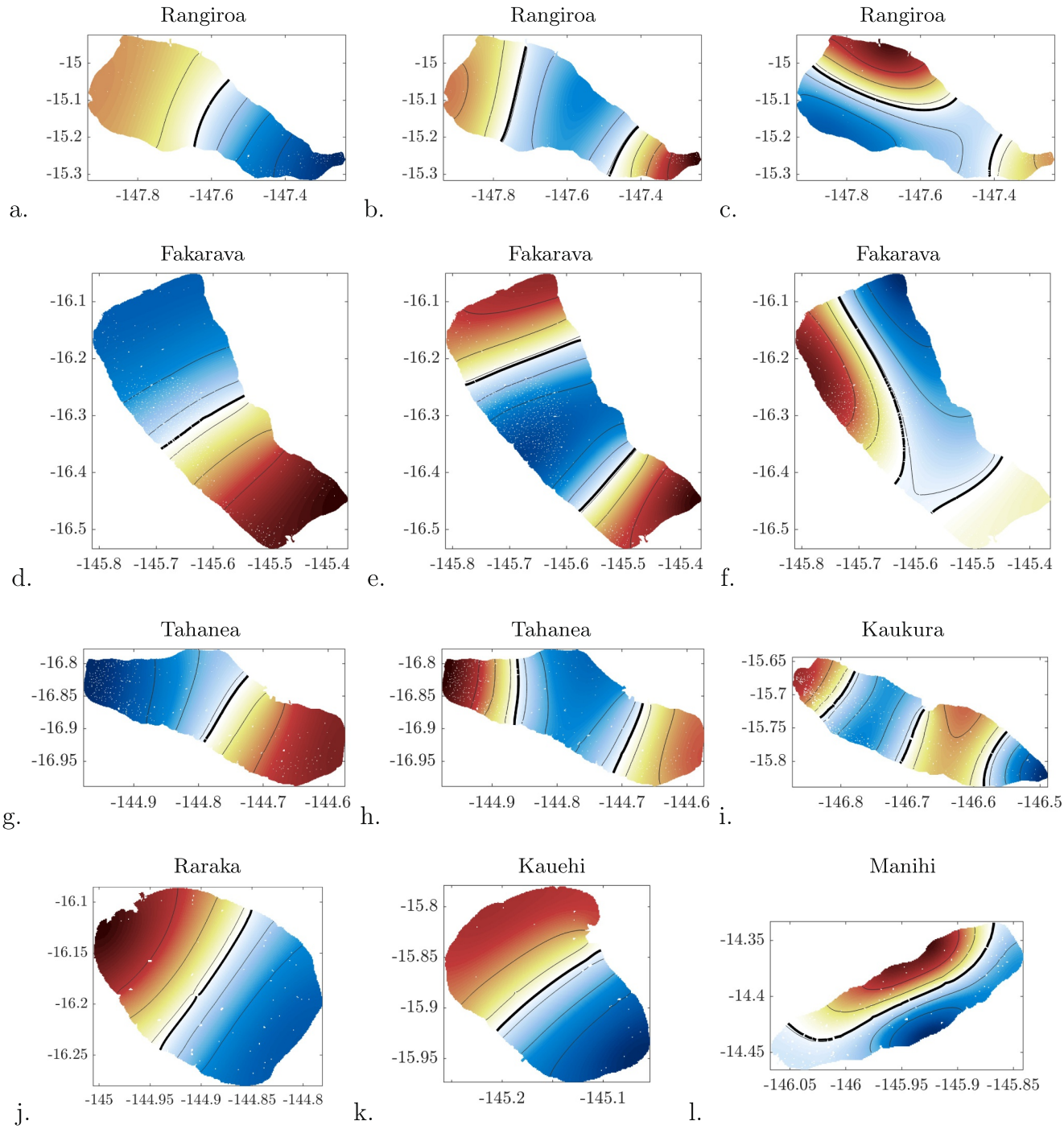

Figure 3. Eigenmodes V_i derived from the model (a,d,g,j,k: V_1; b,e,h: V_2; f,i: V_3; c,l: V_4). Same lagoons as in Figure 2. Opposite signs of elevation are shown in red and blue, with nodal lines highlighted in thick black. The colorbar, centered on 0 (white shading), is not provided as eigenmodes are defined up to a multiplicative constant. Thin black lines correspond to iso-contours.

Figure 4d, computed from P_1, which is located on or very near a nodal line for these modes (Figures 5b and 5d). The remaining lagoon spectra are available in Figure S6 in Supporting Information S1. All 7 lagoon sensors agree on the nodal line positions and consistently identify the periods of the first 4 modes listed in Figure 4g when detected.

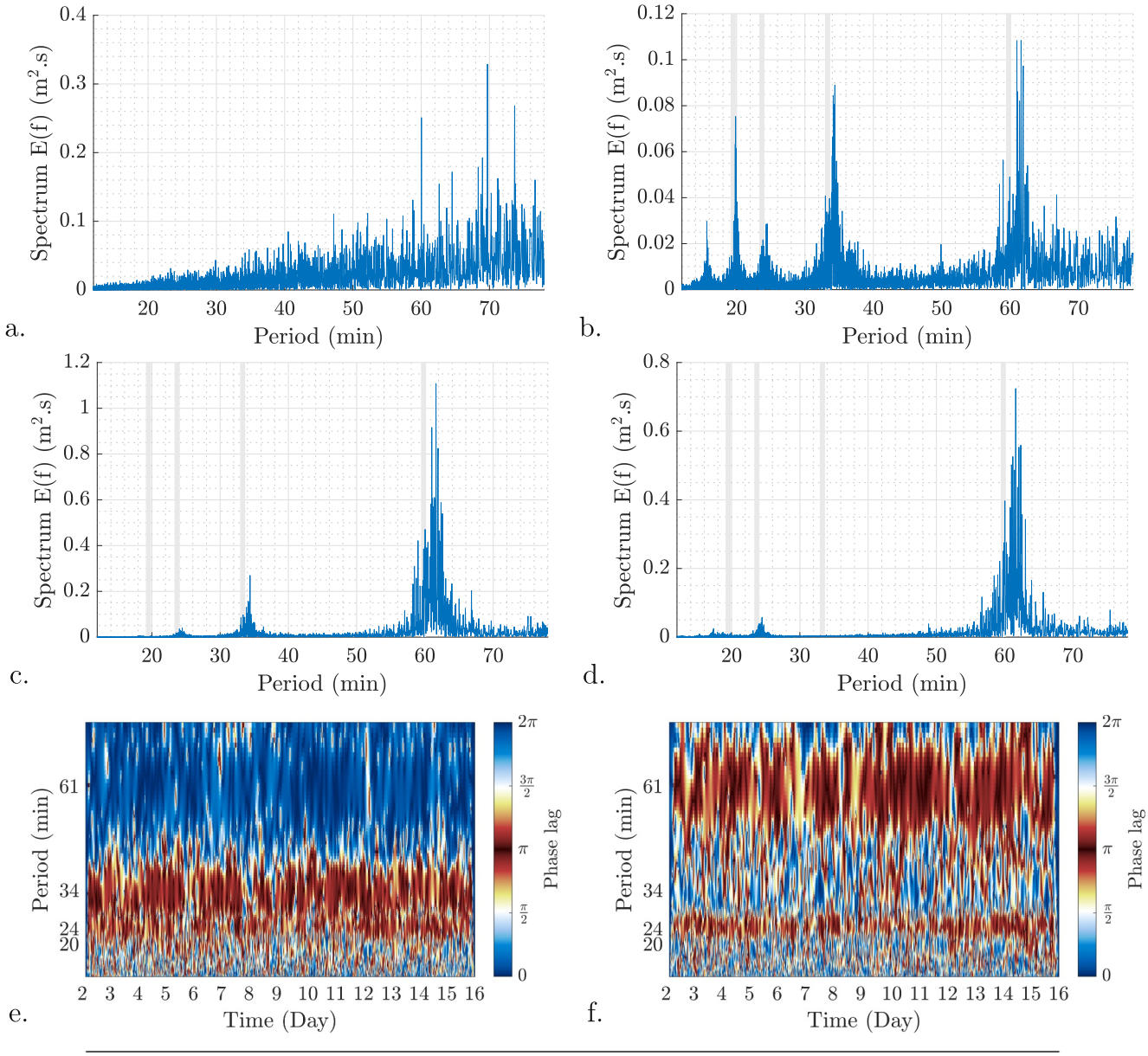

g.

Seiche modes	Mode 1	Mode 2	Mode 3	Mode 4
Predicted (model)	59.8	33.3	23.7	19.5
Measured (pressure sensors)	61	34	24	20

Figure 4. Spectral analyses of pressure sensor measurements. Panels (a) to (d): power spectral density estimates from P_9 (a, ocean), P_3, P_7 and P_1 (b–d respectively, lagoon). Panels (e) and (f): Hovmöller diagram of phase lags $\phi_{3,7}$ (e) and $\phi_{3,1}$ (f); blue indicates signals in phase, while red denotes phase opposition; the numbers on the *x*-axis represent the day of April. Panel (g): period of the 4 first seiche modes of Raroia, in minutes. Model-predicted periods are indicated by gray lines in panels (b)–(d).

Seiche geometry analysis from the pressure sensors can be extended by examining phase lags. Phase lags are derived from Continuous Wavelet Transform (see Section 2.3). They are displayed in Figures 4e and 4f as Hovmöller diagrams over the period band of 12 − 78 min (*y*-axis) throughout the first 2 weeks of measurements (*x*-axis). Figure 4e (resp. 4f) shows the phase lag $\phi_{3,7}$ (resp. $\phi_{3,1}$) between sensors P_3 and P_7 (resp. P_1), which correspond to the central and southernmost (resp. northernmost) sensors in the lagoon. Distinct horizontal bands emerge around the first three seiche periods (60, 34 and 24 min). Blue indicates in-phase relationships, while red

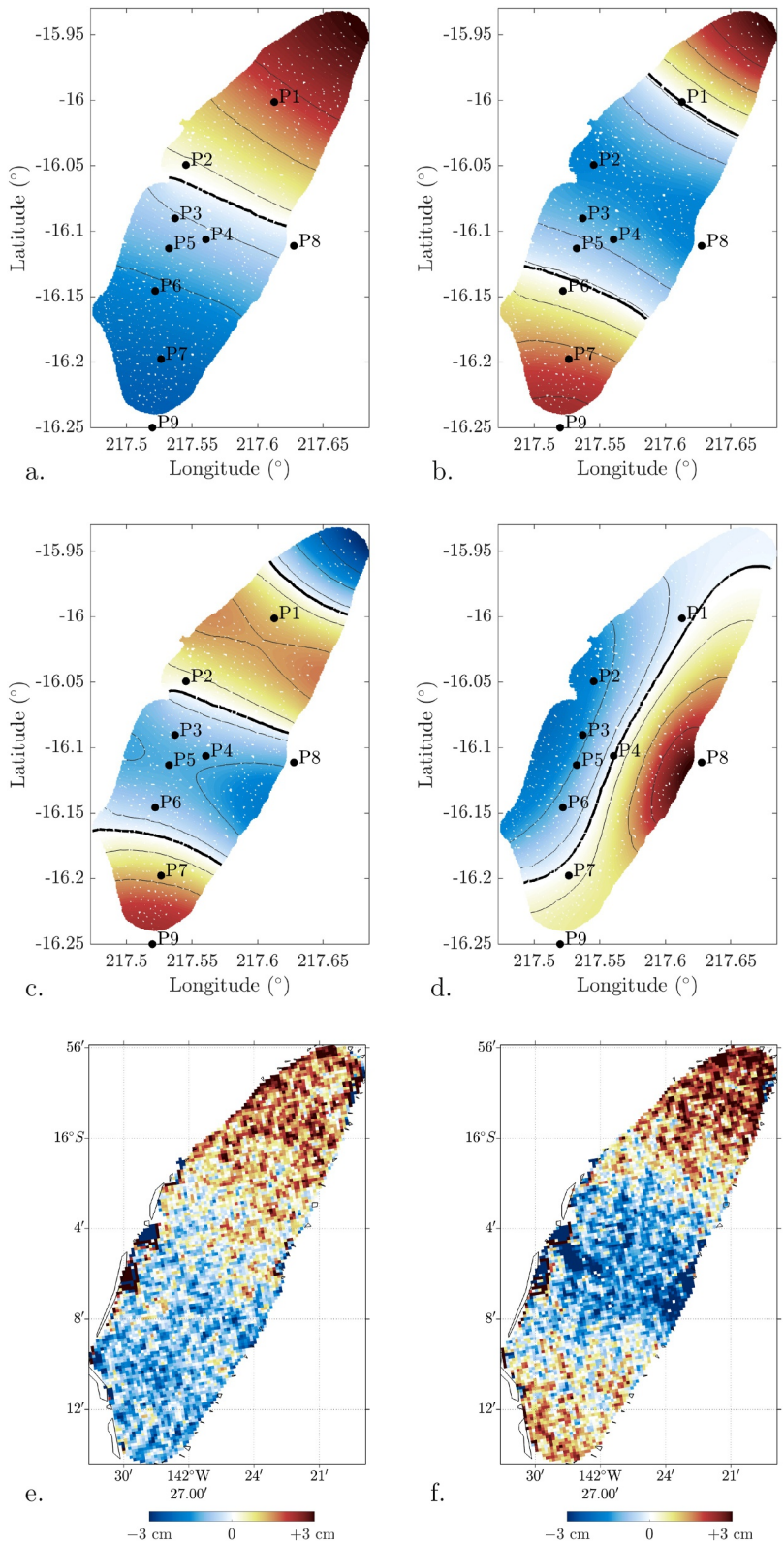

Figure 5. Geometries of seiche modes in the Raroia lagoon. Panels (a) to (d): modes 1 to 4 modeled from Raroia bathymetry; the associated periods are provided in Figure 4g. Pressure sensor locations are superimposed. Panels (e) and (f): SSH anomaly reconstructed from KaRIn SSH measurements in Raroia during SWOT Cal/Val phase on (e) 21 April and (f) 8 April 2023. The colorbar spans 6 cm and is centered on the median SSH anomaly within the lagoon.

denotes phase opposition, corresponding respectively to even and odd numbers of nodal lines between the two sensors. The blue band around the first-mode period (60 min) in Figure 4e is consistent with the modeled geometry (Figure 5a), in which P_3 and P_7 are not separated by any nodal line. Similarly, the phase opposition between P_3 and P_7 at the periods of the second and third modes (34 and 24 min, Figure 4e), as well as the phase opposition between P_1 and P_3 for modes 1 and 3 (60 and 24 min, Figure 4f), align with Figures 5a–5c, according which one nodal line separates the respective sensors at the corresponding modes. No clear in-phase or out-of-phase relationship emerges between P_1 and P_3 for mode 2 (34 min, Figure 4f), as P_1 lies on its nodal line (Figure 5b). Likewise, all phase lags measured from the lagoon sensors are consistent with the model-predicted nodal line positions, relative to the sensor locations, for modes 1, 2, and 3 (see Figure S8 in Supporting Information S1 for the remaining Hovmöller diagrams).

Besides in situ observations, nearly 150 KaRIn measurements of SSH anomalies are currently available for this lagoon (about 100 more than for other lagoons). A dozen of these exhibit seiche-like patterns; two representative cases are shown in Figures 5e and 5f. The SSH anomaly in Figure 5e exhibits the structure of a mode 1 oscillation as computed by the model (Figure 5a), while Figure 5f is very similar to mode 2 (Figure 5b). Higher harmonics (modes 3 in Figure 5c and 4 in Figure 5d) were not observed, probably because of their weaker amplitude.

5. Discussion

This study investigates the presence of seiches in French Polynesia lagoons using SWOT satellite altimetry, in situ measurements and idealized modeling. We show that the data from the KaRIn instrument onboard SWOT provide an unprecedented description of seiche oscillation modes within lagoons. The geometries visible in images of the SWOT SSH anomaly exhibit similar structures to the modes computed with an eigenvalue model based on the shallow-water equations. The model has been successfully compared to a network of pressure sensors deployed in the Raroia lagoon, located on SWOT's Cal/Val orbit. Despite the approximations used in the model, particularly regarding bathymetry and boundary conditions, the seiche periods and the locations of the nodelines show remarkable agreement with the in situ measurements. The two sensors placed on the outer reef highlight that these periods are typical of the lagoon, further confirming that they correspond to the lagoon's eigenmodes.

Further studies will be needed to uncover the exciting mechanism for seiche-modes at the scale of an atoll. These are free eigenmodes, which can be excited—much as a guitar string or a drumhead—by a localized perturbation (such as an atmospheric disturbance related to a storm, or an oceanic forcing, including large swells). Understanding how and why these large-scale modes, and their harmonics, are excited will require further theoretical and observational studies.

Observations of large scale modes such as those on Figures 2, 5e, and 5f are unprecedented and only made possible thanks to SWOT's innovative technology. Conventional nadir altimetry missions (such as Jason or Sentinel-3) do not provide direct 2D SSH observations. In addition, gridded multi-mission products combining data from these altimeters offer 2D sea level anomaly fields on a global grid with a typical spatial resolution of $0.25° \times 0.25°$. For comparison, the largest Polynesian lagoon, Rangiroa, spans less than $1° \times 0.5°$ in longitude and latitude.

In situ sensors are highly valuable for measuring the temporal behavior of seiche modes but comparatively offer less insight into their spatial structure. In addition, deploying such a network in highly remote locations like the Raroia atoll is technically challenging. SWOT thus provides a unique and highly valuable complement to in situ observations in lagoons, in order to investigate how long-period modes affect reef islands and their connection to submersion risks.

Conflict of Interest

The authors declare no conflicts of interest relevant to this study.

Data Availability Statement

The SWOT L2 and L3 LR SSH KaRIn products used in this study are available on the Aviso website: https://www.aviso.altimetry.fr/en/data/products/sea-surface-height-products/global/swot-karin-low-rate-ocean-produ

cts.html and https://www.aviso.altimetry.fr/en/data/products/sea-surface-height-products/global/swot-l3-ocean-products.html. They correspond to L2 Expert version PGC0 (SWOT, 2023), L3 Expert version 2.0.1 (SWOT, 2024a) and L3 Unsmoothed version 2.0.1 (SWOT, 2024b) products. The lagoon contours are freely available on the open public data platform TeFenua under open licence Etalab 2.0: https://arcg.is/0jP5u00. The bathymetry fields are available upon request to the DRM (Polynesia's Direction of Marine Ressources). Most of them were carried out within the framework of the ANR-funded MANA (Management of Atolls) project. The ERA5 surface pressure data are available on the Climate Data Store catalogue (Hersbach et al., 2023).

Acknowledgments
This work was supported by CNES/TOSCA (Maeva project) and the "Institut des Mathématiques pour la Planète Terre." We warmly thank Lin Sheng for making the deployment of pressure sensors in Raroia possible. Logistical support from CRIOBE was also essential. We also thank Pascal Bonnefond and Olivier Lafitte for insightful discussions as well as Xavier Bertin, Valérie Ballu and the ANR PIA3 Equipex + MARMOR project for providing three RBR sensors.

References

Andréfouët, S., Chauvin, C., Spraggins, S., Torres-Pulliza, D., & Kranenburg, C. (2005). *Atlas des récifs coralliens de polynésie française*. IRD.

Andréfouët, S., Genthon, P., Pelletier, B., Le Gendre, R., Friot, C., Smith, R., & Liao, V. (2020). The lagoon geomorphology of pearl farming atolls in the central Pacific Ocean revisited using detailed bathymetry data. *Marine Pollution Bulletin*, *160*, 111580. https://doi.org/10.1016/j.marpolbul.2020.111580

Audusse, E., Lafitte, O., Leroy, A., Mélinand, B., Pham, C.-T., & Quemar, P. (2017). Parametric study of the accuracy of an approximate solution for the mild-slope equation. In *2017 19th international symposium on symbolic and numeric algorithms for scientific computing (synasc)* (pp. 79–85). https://doi.org/10.1109/SYNASC.2017.00024

Bechle, A. J., Kristovich, D. A. R., & Wu, C. H. (2015). Meteotsunami occurrences and causes in lake michigan. *Journal of Geophysical Research: Oceans*, *120*(12), 8422–8438. https://doi.org/10.1002/2015JC011317

Cheriton, O. M., Storlazzi, C. D., & Rosenberger, K. J. (2016). Observations of wave transformation over a fringing coral reef and the importance of low-frequency waves and offshore water levels to runup, overwash, and coastal flooding. *Journal of Geophysical Research: Oceans*, *121*(5), 3121–3140. https://doi.org/10.1002/2015JC011231

Emery, W. J., & Thomson, R. E. (2001). Chapter 5 - Time-series analysis methods. In W. J. Emery & R. E. Thomson (Eds.), *Data analysis methods in physical oceanography (revised* (2nd ed.) (Revised Second Edition ed., pp. 371–567). Elsevier Science. https://doi.org/10.1016/B978-044450756-3/50006-X

Fu, L.-L., Pavelsky, T., Cretaux, J.-F., Morrow, R., Farrar, J. T., Vaze, P., et al. (2024). The surface water and ocean topography mission: A breakthrough in radar remote sensing of the ocean and land surface water. *Geophysical Research Letters*, *51*(4), e2023GL107652. https://doi.org/10.1029/2023GL107652

Gawehn, M., van Dongeren, A., van Rooijen, A., Storlazzi, C. D., Cheriton, O. M., & Reniers, A. J. H. M. (2016). Identification and classification of very low frequency waves on a coral reef flat. *Journal of Geophysical Research: Oceans*, *121*(10), 7560–7574. https://doi.org/10.1002/2016JC011834

Hersbach, H., Bell, B., Berrisford, P., Biavati, G., Horányi, A., Muñoz Sabater, J., et al. (2023). Era5 hourly data on single levels from 1940 to present [dataset]. *Copernicus Climate Change Service (C3S) Climate Data Store (CDS)*. https://doi.org/10.24381/cds.adbb2d47

Lenhardt, X. (1991). Hydrodynamique des lagons d'atoll et d'île haute en polynésie française (Doctoral dissertation, Muséum National d'Histoire Naturelle de Paris, Paris, France). Retrieved from https://horizon.documentation.ird.fr/exl-doc/pleins_textes/pleins_textes_2/etudes_theses/34233.pdf

Levitin, M., Mangoubi, D., & Polterovich, I. (2023). *Topics in spectral geometry* (Vol. 237). American Mathematical Society.

Matson, M., & Berg, C. P. (1981). Satellite detection of seiches in great salt lake, utah. *JAWRA Journal of the American Water Resources Association*, *17*(1), 122–128. https://doi.org/10.1111/j.1752-1688.1981.tb02595.x

Metzner, M., Gade, M., Hennings, I., & Rabinovich, A. B. (2000). The observation of seiches in the baltic sea using a multi data set of water levels. *Journal of Marine Systems*, *24*(1–2), 67–84. https://doi.org/10.1016/s0924-7963(99)00079-2

Monahan, T., Tang, T., Roberts, S., & Adcock, T. A. A. (2025). Observations of the seiche that shook the world. *Nature Communications*, *16*(1), 4777. https://doi.org/10.1038/s41467-025-59851-7

Morrow, R., Fu, L.-L., Ardhuin, F., Benkiran, M., Chapron, B., Cosme, E., et al. (2019). Global observations of fine-scale ocean surface topography with the Surface Water and Ocean Topography (SWOT) mission. *Frontiers in Marine Science*, *6*, 232. https://doi.org/10.3389/fmars.2019.00232

Péquignet, A. C. N., Becker, J. M., Merrifield, M. A., & Aucan, J. (2009). Forcing of resonant modes on a fringing reef during tropical storm man-yi. *Geophysical Research Letters*, *36*(3), L03607. https://doi.org/10.1029/2008GL036259

Pomeroy, A. W. M., Van Dongeren, A., Lowe, R., de Vries, J. v. T., & Roelvink, J. (2012). Low frequency wave resonance in fringing reef environments. *Coastal Engineering Proceedings*, *33*, 25. https://doi.org/10.9753/icce.v33.currents.25

Rabinovich, A. (2009). In Y. C. Kim (Ed.), *Seiches and harbor oscillations*. World Scientific Publishing Co. https://doi.org/10.1142/9789812819307_0009

Seo, J. Y., Choi, B.-J., Choi, S. M., Ryu, J., & Ha, H. K. (2024). Contribution of coastal seiches to sediment transport in a microtidal semi-enclosed Bay. *Frontiers in Marine Science*, *11*, 1392435. https://doi.org/10.3389/fmars.2024.1392435

Shimozono, T., Tajima, Y., Kennedy, A. B., Nobuoka, H., Sasaki, J., & Sato, S. (2015). Combined infragravity wave and sea-swell runup over fringing reefs by super typhoon haiyan. *Journal of Geophysical Research: Oceans*, *120*(6), 4463–4486. https://doi.org/10.1002/2015JC010760

Sous, D., Tissier, M., Rey, V., Touboul, J., Bouchette, F., Devenon, J.-L., et al. (2019). Wave transformation over a barrier reef. *Continental Shelf Research*, *184*, 66–80. https://doi.org/10.1016/j.csr.2019.07.010

SWOT. (2023). SWOT Level-2 KaRIn Low Rate SSH Expert (v2.0) [dataset]. https://doi.org/10.24400/527896/A01-2023.015

SWOT. (2024a). SWOT Level-3 KaRIn Low Rate SSH Expert (v2.0.1) [dataset]. https://doi.org/10.24400/527896/A01-2023.018

SWOT. (2024b). SWOT Level-3 KaRIn Low Rate SSH Unsmoothed (v2.0.1) [dataset]. https://doi.org/10.24400/527896/A01-2024.003

Wilson, B. (1972). *Seiches*. Academic Press.

Winter, G., Lowe, R. J., Symonds, G., Hansen, J. E., & van Dongeren, A. R. (2017). Standing infragravity waves over an alongshore irregular rocky bathymetry. *Journal of Geophysical Research: Oceans*, *122*(6), 4868–4885. https://doi.org/10.1002/2016JC012242

Zheng, Q., Hu, J., Zhu, B., Feng, Y., Jo, Y.-H., Sun, Z., et al. (2014). Standing wave modes observed in the south China sea deep basin. *Journal of Geophysical Research: Oceans*, *119*(7), 4185–4199. https://doi.org/10.1002/2014JC009957

References From the Supporting Information

Aucan, J., Desclaux, T., Gendre, R. L., Liao, V., & Andréfouët, S. (2021). Tide and wave driven flow across the rim reef of the atoll of raroia (tuamotu, French Polynesia). *Marine Pollution Bulletin*, *171*, 112718. https://doi.org/10.1016/j.marpolbul.2021.112718

Codiga, D. L. (2011). *Unified tidal analysis and prediction using the UTide MATLAB functions Tech. Report*. Graduate School of Oceanography, University of Rhode Island.

Defant, A. (1960). *Physical oceanography* (Vol. 2). Pergamon Press.

Forel, F.-A. (1876). La formule des seiches. *Archives des Sciences Physiques et Naturelles*, 1–15.

Gao, J., Zhou, X., Zhou, L., Zang, J., Chen, Q., & Ding, H. (2018). Numerical study of harbor oscillations induced by water surface disturbances within harbors of constant depth. *Ocean Dynamics*, *68*(12), 1663–1681. https://doi.org/10.1007/s10236-018-1222-0

Priya, P., Kumar, P., & Rajni (2024). Mathematical modelling of arbitrary shaped domain based on dual reciprocity boundary element method with variable bathymetry. *Ocean Engineering*, *308*, 118366. https://doi.org/10.1016/j.oceaneng.2024.118366

Rueda, F. J., & Schladow, S. G. (2002). Surface seiches in lakes of complex geometry. *Limnology & Oceanography*, *47*(3), 906–910. https://doi.org/10.4319/lo.2002.47.3.0906